Catalytic Properties of Perovskite-type Mixed Oxides, $La_{1-x}Sr_xCoO_3$

Teiji NAKAMURA, Makoto MISONO,* and Yukio YONEDA

Department of Synthetic Chemistry, Faculty of Engineering, The University of Tokyo, Hongo, Bunkyo-ku, Tokyo 113

(Received June 8, 1981)

The reactivity and related properties of oxygen both in the bulk and on the surface has been investigated for perovskite-type mixed oxides ($La_{1-x}Sr_xCoO_3$), in regard to the effects of Sr^{2+}-substitution and calcination temperature. The reducibility and the readiness of oxygen desorption increased with the Sr^{2+} content, x, but the re-oxidation became slower with x. These results have been explained on the basis of the change in the chemical potential of lattice oxygen. The diffusivity of oxygen in the bulk and the ability to activate the oxygen molecule also increased with x. Oxygen vacancies in the bulk and on the surface, which tended to increase with x, are likely responsible for these reactions. The release of oxygen from the bulk became more difficult as the calcination temperature increased, in conformity with the trend of the catalytic activity.

For the design of catalysts, it is very helpful to know the relationships between the solid state chemistry of catalysts and the catalytic properties, that is, the structure-property relationships. It is, therefore, desirable to study catalyst materials of which the structure is well defined and for which the surface or bulk properties can be continuously or stepwise changed without affecting the fundamental structure of the catalyst.

Perovskite-type mixed oxides (ABO_3) are typical examples suitable for this purpose, since their structures have been satisfactorily clarified and their electronic properties can be modified in various ways by the substitution of the constituting elements.[1] For example, the oxidation state of the B-site ion and the number of oxygen defects can be controlled by introducing a divalent ion in the A-site. Futhermore, perovskite-type mixed oxides are important catalysts in practical processes such as oxidation,[2,3] NO elimination[4,5] and hydrogenolysis.[6] It has already been reported that the perovskite-type mixed oxides are very active in complete oxidation reactions.[7,8]

We found previously that $La_{1-x}Sr_xCoO_3$ (x=0—0.4) showed high catalytic activity for the oxidation of C_3H_8, CH_4, and CO.[8] Among them, $La_{0.8}Sr_{0.2}CoO_3$ calcined at 850 °C was the most active, and its activity was comparable with or greater than that of Pt, Pd, and Ni catalysts. However, there have been few studies on the reaction mechanism and the reactivity of oxygen species of the perovskite-type mixed oxides, in relation to the catalytic activity for oxidation reactions.

Oxygen species responsible for the oxidation reaction have been well clarified, for example, in the case of Bi_2O_3–MoO_3[9] and γ-Fe_2O_3.[10] Both are active catalysts for allyl-type oxidation of olefins, in which lattice oxygen is responsible for catalysis. Reduction and oxidation of the whole bulk of these catalysts proceed readily under the reaction conditions, by the diffusion of lattice oxygen for Bi_2O_3–MoO_3 or metal cation for γ-Fe_2O_3. The diffusion of the cation or anion appears very important for allyl-type oxidation. As for the perovskite-type mixed oxide, it is only reported in the field of electrochemistry that the oxygen diffusion in $Nd_{1-x}Sr_xCoO_3$ is more rapid than that in ordinary metal oxides.[11] In the present work we studied the reactivity and diffusivity of oxygen in $La_{1-x}Sr_xCoO_3$, in order to clarify the relationships between these properties and the catalytic action. We studied particularly the effects of Sr^{2+}-substitution and the calcination temperature on the reactivity and related properties of oxygen, both in the bulk and on the surface.

Experimental

Catalysts. The catalysts were prepared from the mixture of metal acetates as described in the previous paper.[8] Powder X-ray diffraction patterns (XRD) were recorded with an X-ray diffractometer (Rigaku Denki, Rotaflex, RU-200) using Cu Kα radiation. All the $La_{1-x}Sr_xCoO_3$ (calcined above 850°C) used in this work showed diffration peaks only of the perovskite-type structure. Some of the samples are non-stoichiometric, $La_{1-x}Sr_xCoO_{3-\lambda}$. This non-stoichiometry and slight change in XRD observed upon reduction will be discussed in the later sections.

Apparatus. Besides conventional pulse and flow reactors, a circulation system (*ca.* 250 cm^3) was used for the reactions. These were the same as described elsewhere.[8,10]

Procedures. *Pulse Reaction*: The reduction of the catalysts by CO was conducted in the pulse reactor. Prior to the reaction, the catalysts (50 mg) were heated in O_2 stream for 1 h at 300 °C. The flow rate of carrier gas (He) was 30 cm^3 min^{-1} and the size of each CO pulse was usually 0.1 cm^3. Products were analyzed by a gas chromatograph (DMS, 5 m, 0 °C, or Porapak Q, 1.5 m, 83 °C).

Isotopic Exchange and Equilibration of O-18: ^{18}O-exchange between O_2 and perovskites and ^{18}O-equilibration of O_2 in the gas phase were conducted in the closed circulation system. Prior to reaction, the samples (300 mg) were treated with pure O_2 (10 kPa) at 300 °C (with circulation and a trap kept at liquid-nitrogen temperature) and subsequently evacuated for 1 h at 300 °C. O_2 enriched in ^{18}O (70 atom%) was purchased from Japan Radioisotope Association.^{18}O-distributions in O_2 in the gas phase was analyzed by a mass spectrometer (Hitachi Co. Ltd., RMU-S) by intermittent sampling.

Temperature Programmed Desorption (TPD) of Oxygen: TPD of oxygen was carried out with a flow system using helium as a carrier gas. Prior to each run, the samples (0.5 g or 1 g) were treated in an O_2 stream for 1 h at 300 °C and cooled to room temperature in the O_2 stream. Then an He stream was substituted for an O_2 stream at room temperature. Oxygen impurity in He was removed by a molecular sieve trap kept at the temperature of liquid nitrogen. Then the temperature of the sample was raised at the constant rate of 20 °C min^{-1} and the oxygen desorbed was detected by use of a quadrupole mass spectrometer (NEVA, NAG-531).

Results

Temperature Programmed Desorption (TPD) of Oxygen. Figure 1 shows TPD of oxygen from $La_{1-x}Sr_xCoO_3$ (x=0—0.6), where the rate of desorption calculated from the O_2 concentration in the eluent gas is plotted against temperature. It is obvious in this figure that the rate and the amount of O_2 desorption increased with the Sr^{2+} content, x. Oxygen desorbed below 600 °C amounted to 5.4 $cm^3\ g^{-1}$ (1.20 $cm^3\ m^{-2}$) for x=0.6, 2.8 $cm^3\ g^{-1}$ (0.519 $cm^3\ m^{-2}$) for x=0.4, 0.6 $cm^3\ g^{-1}$ (0.14 $cm^3\ m^{-2}$) for x=0.2, and 0.07 $cm^3\ g^{-1}$ (0.028 $cm^3\ m^{-1}$) for x=0. The amounts for x=0.4 and 0.6 corresponded to several layers of oxygen. These desorptograms of x=0—0.4 were reproducible after the heat treatment in an O_2 stream at 300 °C for 1 h. In the case of x=0.6 it was not completely reversible by this treatment, indicating that the rate of re-oxidation for x=0.6 was not rapid enough. For x=0.6, an O_2-treatment longer than 2 h at 300 °C was necessary to reproduce the initial desorptogram.

Figure 2 shows TPD of oxygen from $La_{0.8}Sr_{0.2}CoO_3$ calcined at 850, 900, and 1200 °C. The amount of oxygen desorbed decreased with the calcination temperature. The shapes of the desorptograms were rather similar: The desorption rate increased sharply at 500—600 °C after initial rises at lower temperatures. However, a significant difference was found in the temperature at which the desorption curves first increased: it was about 200 °C for $La_{0.8}Sr_{0.2}CoO_3$ calcined at 850 °C, about 250 °C for 900 °C-calcined sample, and about 350 °C for a 1200 °C-calcined sample. This result demonstrates that the release of oxygen from the bulk of $La_{1-x}Sr_xCoO_3$ becomes more difficult as the calcination temperature increased, even though the catalysts had the same composition.

It is to be noted that the increase in the readiness of oxygen desorption with increasing x was also found for 1200 °C-calcined samples.

Reversible Adsorption of Oxygen. Figure 3 shows the adsorption of oxygen for x=0 and 0.2 measured in the static system (P_{O_2}=10—20 Torr**). The samples were pre-evacuated for 0.5 h at each temperature. The adsorption isotherms exhibited saturation at about 10 Torr. The amount of adsorption increased with

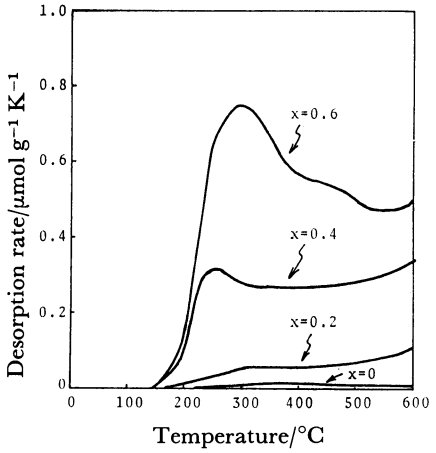

Fig. 1. TPD curves of oxygen from $La_{1-x}Sr_xCoO_3$ (x=0—0.6). Rate of temperature increase (β)=20 °C min^{-1}.

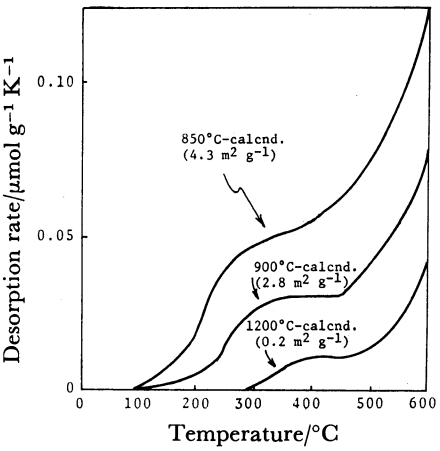

Fig. 2. TPD curves of oxygen from $La_{0.8}Sr_{0.2}CoO_3$ calcined at 850, 900, and 1200 °C. Rate of temperature increase (β)=20 °C min^{-1}.

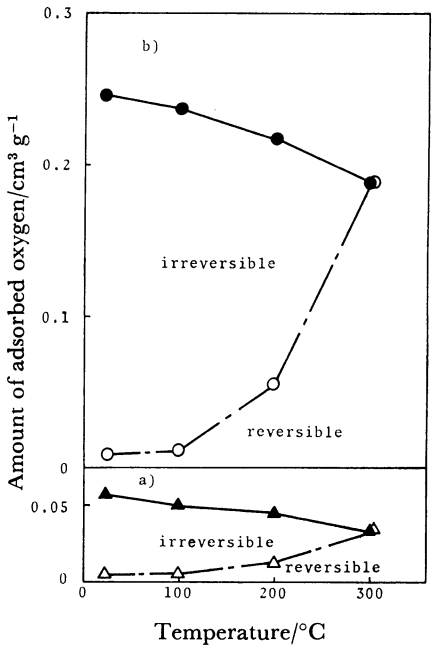

Fig. 3. Adsorption (or absorption) of oxygen by $LaCoO_3$ (a) and $La_{0.8}Sr_{0.2}CoO_3$ (b).
After the catalysts were evacuated at 300 °C for 0.5 h, O_2 was introduced at 300 °C. The solid symbols (▲, ●) at 300 °C represent the amounts of oxygen adsorbed at this stage. Then, the samples were cooled to 200, 100, and 25 °C stepwisely in the presence of O_2 (*ca.* 10 Torr). Solid symbols at each temperature express the cumulative amount of adsorbed oxygen. Open symbols (△, ○) are the amounts of oxygen which were reversibly adsorbed at each temperature. Therefore, the differences between the solid and open symbols are the irreversibly adsorbed oxygen at each temperature.

** 1 Torr≈133.3 Pa.

temperature, and the reversible adsorption of oxygen at room temperature was very small. If one assumes the value of δ to be null at room temperature, the values of δ are calculated to be 0.0049 (after 300 °C-evac.), 0.0012 (at 300 °C in O_2) for $x=0.2$, and 0.0011 (after 300 °C-evac.), 0.00046 (at 300 °C in O_2) for $x=0$.

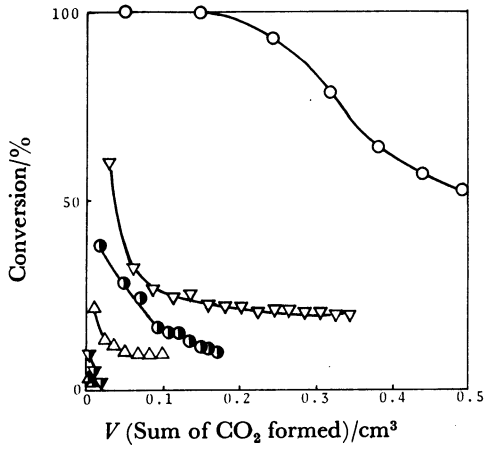

Fig. 4. Reduction by CO pulse at 200 and 300 °C.
▲: $LaCoO_3$, ◑: $La_{0.8}Sr_{0.2}CoO_3$, ▼: $La_{0.8}Ce_{0.2}CoO_3$ at 200 °C, △: $LaCoO_3$, ○: $La_{0.8}Sr_{0.2}CoO_3$, ▽: $La_{0.8}Ce_{0.2}CoO_3$ at 300 °C.
Catal. wt: 50 mg, CO pulse size: 0.1 cm³.

Reducibility of Catalysts by CO (Pulse Method). Figure 4 shows results of reduction by CO pulses at 200 and 300 °C. The ordinate indicates the conversion of each CO pulse to CO_2, and the abscissa is the sum of CO_2 formed from the pulse and the preceding pulses, which expresses the extent of the reduction of the catalysts. It is noted that $La_{0.8}Sr_{0.2}CoO_3$ was reduced more easily than $LaCoO_3$ and $La_{0.8}Ce_{0.2}CoO_3$. Even after oxygen molecules corresponding to several layers of surface were removed, the reducibility maintained a high level for $La_{0.8}Sr_{0.2}CoO_3$.

This fact indicates that the rate of oxygen supply from the bulk to the surface is very rapid in the case of $La_{0.8}Sr_{0.2}CoO_3$. Rapid diffusion of bulk oxide ion to the surface is further demonstrated by the effect of CO-pulse size on the rate of reduction (Fig. 5). CO was converted completely to CO_2 at 300 °C up to the pulse size of 0.3 cm³, while the formation of CO_2 was almost saturated at 0.1—0.2 cm³ at 150 °C. Since the oxide ion on the surface (by assuming 0.96×10^{19} atom m^{-2} for one surface layer) corresponds to 0.1 cm³ of CO_2, this result demonstrates that the rate of oxygen supply is very fast at 300 °C.

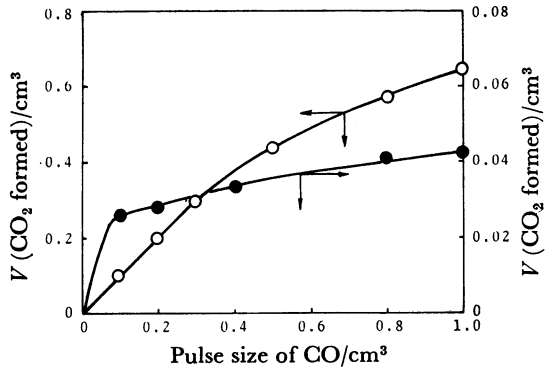

Fig. 5. Effect of pulse size on CO reduction of $La_{0.8}Sr_{0.2}CoO_3$ at 150 and 300 °C.
●: 150 °C, ○: 300 °C.

$LaCoO_3$ was much less reducible than $La_{0.8}Sr_{0.2}CoO_3$. $La_{0.8}Ce_{0.2}CoO_3$ appeared a little more reducible than $LaCoO_3$. However, the difference is small when normalized to the surface area. The conversion of the first CO pulse at 150 °C given in Table 1 demonstrates clearly the trend that the reducibility increases with the Sr^{2+} content.

Table 1. Reduction of $La_{1-x}Sr_xCoO_3$ by CO[a] at 150 °C

x	Conversion/% CO→CO_2
0	1
0.2	25
0.4	77
0.6	100

a) Pulse size of CO: 0.1cm³.

Re-oxidation of the Reduced Catalysts. When O_2 was pulsed at 300 °C over $LaCoO_3$ and $La_{0.8}Sr_{0.2}CoO_3$ which had been reduced by CO pulses, these catalysts absorbed O_2 until its amount became equivalent to that removed in the preceding reduction, that is, the reduction and re-oxidation cycle was stoichiometric and reversible for these two catalysts. However, in the case of $La_{0.6}Sr_{0.4}CoO_3$ and $La_{0.4}Sr_{0.6}CoO_3$, the reduced catalysts were not fully re-oxidized by O_2 pulse at 300 °C. For example, $La_{0.4}Sr_{0.6}CoO_3$ (reduced by 3%) absorbed 74% of the stoichiometric amount of oxygen. This trend was enhanced at lower temperatures. At 150 °C $La_{0.6}Sr_{0.4}CoO_3$ (3% reduced) absorbed only 19% and $La_{0.4}Sr_{0.6}CoO_3$ (3% reduced) only 10%. The rate of re-oxidation tended to be faster when the catalyst was pre-reduced to a greater extent.

Structural Changes Accompanying the Reduction and Re-oxidation. Changes in XRD upon reduction and

Table 2. Changes in XRD of $La_{1-x}Sr_xCoO_3$ by reduction[a]

Distance of lattice planes/Å					
$x=0$		$x=0.2$		$x=0.6$	
i[b]	ii[c]	i[b]	ii[c]	i[b]	ii[c]
3.82	3.86	3.82	3.89	3.83	3.85
	2.77				2.77
2.71	2.74	2.71	2.74	2.71	2.72
2.68	2.71				
2.22	2.23	2.21	2.24	2.21	2.22
2.18	—	2.19	2.22		
					2.06
	1.94				1.94
1.91	1.92	1.91	1.93	1.91	1.92

a) About 5% reduced by CO at 400 °C. b) Before reduction. c) After reduction.

re-oxidation are summarized in Table 2. When the catalysts were reduced by about 5% by CO pulses at 400 °C (to $La_{1-x}Sr_xCoO_{2.85}$ if the sample was $La_{1-x}Sr_xCoO_3$ in the initial state), the diffraction peaks shifted about 0.2—0.5° (2θ) to lower angles. In addition to this shifts, new weak peaks (1.94, 2.06, 2.77 Å) appeared in the case of $LaCoO_3$ and $La_{0.4}Sr_{0.6}CoO_3$. The reduction and re-oxidation of the catalysts are reversible and the structure of the catalysts did not change significantly with reduction.

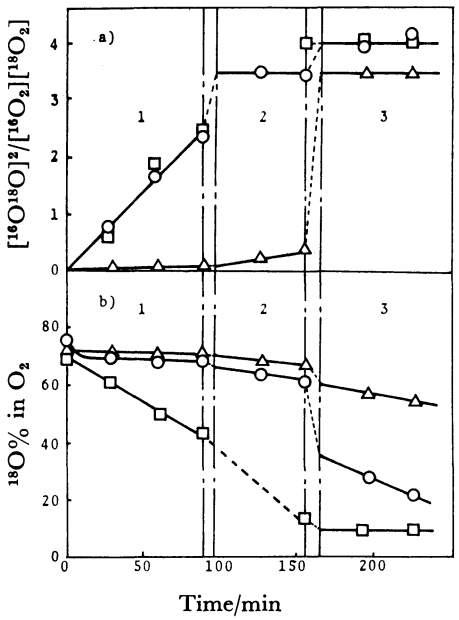

Fig. 6. Isotopic exchange of oxygen.
a): Equilibration, b) Exchange between gaseous and lattice oxygen.
React temp, 1; 150, 2; 200, 3; 300 °C.
△: $LaCoO_3$, ○: $La_{0.8}Sr_{0.2}CoO_3$, □: $La_{0.4}Sr_{0.6}CoO_3$.

Isotopic Equilibration and Exchange of Oxygen. Results of isotopic equilibration and exchange are shown in Fig. 6. The reaction was carried out at three different temperatures for each sample in a successive manner without replacing the gas mixture. The times required to increase the reaction temperature from 150 to 200 °C and 200 to 300 °C were 10 and 15 min, respectively. As shown in Fig. 6a, the isotopic equilibration over $La_{0.8}Sr_{0.2}CoO_3$ and $La_{0.4}Sr_{0.6}CoO_3$ proceeded rapidly at 150 °C, and the value of $[^{16}O^{18}O]^2/[^{16}O_2][^{18}O_2]$ was close to 4 at 200 and 300 °C, the value expected at equilibrium. On the other hand, the equilibration was slow over $LaCoO_3$ even at 200 °C. Figure 6b shows the results of isotopic exchange between lattice oxygen and gaseous oxygen. The rate of exchange on $LaCoO_3$ and $La_{0.8}Sr_{0.2}CoO_3$ was slow at 150 and 200 °C, but it became considerably more rapid at 300 °C. Over $La_{0.4}Sr_{0.6}CoO_3$ both reactions proceeded much more rapidly. In this case about 1.01 cm^3 of oxygen was absorbed just after the introduction of oxygen at 150 °C, indicating that desorption of oxygen was significant during the evacuation at 300 °C prior to the reaction. The ^{18}O-content in O_2 after 1 h at 300 °C was 8.4%. This value was not far from 6.5%, which is expected for complete mixing of lattice oxygen and gaseous oxygen.

Discussion

Structure and Stoichiometry of $La_{1-x}Sr_xCoO_3$ Catalysts. It was previously reported that $La_{1-x}Sr_xCoO_3$ formed perovskite structure when x did not exceed 0.8.[12] But according to a recent report,[13] this system forms a complete solid solution in the whole range of x. A slight distortion to rhombohedral exists in $LaCoO_3$, but it decreases gradually as the Sr^{2+} content, x, increases, and above $x=0.6$ the structure becomes cubic.[12] In spite of this distortion the crystal structures are essentially identical and there is only a small variation in the lattice constant of the pseudo cubic cell from 3.82 Å for $LaCoO_3$ to 3.84 Å for $SrCoO_3$.[14] In accordance with these results, the $La_{1-x}Sr_xCoO_3$ used in the present work all showed the perovskite structure.

When Sr^{2+} is partly substituted for La^{3+}(A-site) of $LaCoO_3$, the oxidation state of Co changes from Co^{3+} to Co^{4+}.[14] Although Co^{4+} was confirmed in $BaCoO_3$[15] $SrCoO_{3-\delta}$[16] and $La_{1-x}Sr_xCoO_{3-\delta}$,[14] it is not stable and tends to be reduced by releasing oxygen. For example, it was reported that the value of δ in $SrCoO_{3-\delta}$ is 0.26 when annealed under 50 bar*** of oxygen at 350 °C and 0.05 under 2000 bar at 300 °C.[16] Therefore, it is probable at a high x value that the charge compensation is accomplished by the formation of oxygen vacancies in addition to the Co^{4+} formation. Actually, according to Jonker *et al.*,[14] Co^{4+} is formed without the formation of oxygen vacancy for $x \leqq 0.4$, but oxygen vacancies are formed besides the Co^{4+} formation when x exceeds 0.4. It was recently confirmed with single crystals that stoichiometric $La_{1-x}Sr_xCoO_3$'s were obtained for $x \leqq 0.2$ by annealing in air.[17] Although the samples used in the present investigation were polycrystalline powders and were mostly calcined at a relatively low temperature, the content of Co^{4+} determined by chemical analysis[15,18] was 20±1% for the sample with $x=0.2$, *i.e.*, $La_{0.8}Sr_{0.2}CoO_{3\pm0.005}$. The sample had been calcined at 850 °C, cooled slowly to 25 °C and then treated in oxygen at 300 °C. Final treatment is the same as the pre-treatment for the catalytic reactions. This result was in agreement with the results reported previously.[14,17] The composition was not determined for $x=0.6$, but it is probably close to $La_{0.4}Sr_{0.6}CoO_{2.925}$ (Co^{4+}: 45%), which was observed by Jonker *et al.*[14] For the single crystals of $x=0.5$, δ was estimated to be 0.077.[17] Consequently, δ of $La_{1-x}Sr_xCoO_{3-\delta}$ catalysts, which were calcined at 850 °C and treated in oxygen at 300 °C, may be close to zero for $x=0$ and 0.2, and 0.075 or slightly smaller for $x=0.6$. This trend in δ with the Sr^{2+} content is thus explained by the instability of Co^{4+}, in other words, the chemical potential of lattice oxygen at a given δ increases with the Sr^{2+} content. As discussed below, the changes with x in the readiness of desorption and reducibility of lattice oxygen are explained by this change in the chemical potential of the lattice oxygen.

*** 1 bar = 10^5 Pa.

Structural Changes during the Redox Cycle. When $La_{1-x}Sr_xCoO_{3-\delta}$ (x=0, 0.2, and 0.6) were reduced by 5% (from δ=0 to 0.15 for x=0 and 0.2, and from *ca.* 0.07 to *ca.* 0.22 for x=0.6) by CO at 400 °C, the diffraction peaks shifted to lower angles and the separation of the lattice planes, d, increased by 0.01—0.05 Å (Table 2). The ionic radius of Co^{3+} is 0.61 Å for high spin state and 0.525 Å for low spin state, while the ionic radius of Co^{4+} is 0.518 Å for $SrCoO_3$[16] and 0.476 Å for 2H-$BaCoO_3$.[19] Therefore, the increase of d on reduction may be due to the difference in the ionic radius between Co^{3+} and Co^{4+}; that is, Co^{4+} changed to Co^{3+} by the reduction. Similar increase in d with δ was reported for $SrCoO_{3-\delta}$ (δ=0.05—0.26).[16] New weak peaks were observed for x=0.6 after reduction besides the shifts of the original diffraction peaks. However, no new peaks were observed for x=0.2, although oxygen vacancies are probably less stable for x=0.2. Therefore, a possible explanation of the new peaks for x=0.6 may be as follows. A Sr-rich phase was present in the sample before reduction and a phase similar to $SrCoO_{2.5}$ was formed by reduction from this Sr-rich phase. $SrCoO_{2.5}$ has the brownmillerite structure, which is closely related to the perovskite structure and there is essentially little difference between these two structures, as discussed above.

For x=0, new weak peaks also appeared by reduction. It was reported that $La_4Co_3O_{10}$ and CoO were formed partially by reduction,[20] but the new peaks for x=0 do not agree with those expected for $La_4Co_3O_{10}$ and the diffraction peaks of CoO were not observed. Although the origin of the new peaks for x=0 is not evident, it is probable that oxygen vacancies are formed by reduction, causing crystal distortion, but it did not lead to decomposition or significant change in the structure. XRD peaks of $La_4Co_3O_{10}$+CoO were not observed for $LaCoO_3$, probably because the degree of reduction in this study (δ=0.15) was smaller than that in the literature (δ=0.26: 1.68 wt%).[20]

The starting perovskite structures were reversibly restored by re-oxidation for all reduced samples. Therefore, the fundamental structure of perovskite was presumably preserved during the redox cycle when the extent of reduction was small as in this study.

Adsorbed Oxygen and Lattice Oxygen. First, the amounts of oxygen desorbed from $La_{1-x}Sr_xCoO_3$ by TPD are compared with those from other metal oxides. CuO and Co_3O_4 are among the oxides showing large values; 1.42×10^{-1} cm^3 m^{-2} for CuO (0.17 m^2 g^{-1}) and 3.30×10^{-2} cm^3 m^{-2} for Co_3O_4 (5.7 m^2 g^{-1}) in the temperature range from 25 °C to 560 °C.[21] The amounts for $La_{1-x}Sr_xCoO_3$ were comparable with (for x=0.2) or much larger (for $x\geqq0.4$) than CuO. The amounts of desorbed oxygen correspond to the increase in δ by 0.012 for x=0.2, 0.051 for x=0.4, and 0.097 for x=0.6. If one assumes the surface oxide density to be 0.96×10^{19} atom m^{-2}, those amounts are about 0.7 surface layers for x=0.2 and several layers for x=0.6. Thus, it is obvious that most of the oxygen desorbed was not the adsorbed oxygen but came from the lattice oxygen.

Oxygen adsorbed after evacuation at a certain temperature was greater than oxygen desorbed in TPD up to the same temperature, indicating that the amount of oxygen desorbed in TPD at each temperature had not reached equilibrium. However, the amount was not very far from the equilibrium value. Therefore, although TPD is governed by the rate, it reflects closely the equilibrium properties. This is in accord with the result in Fig. 7, where the second TPD after the interruption mostly reproduced the rest of TPD conducted without the interruption.

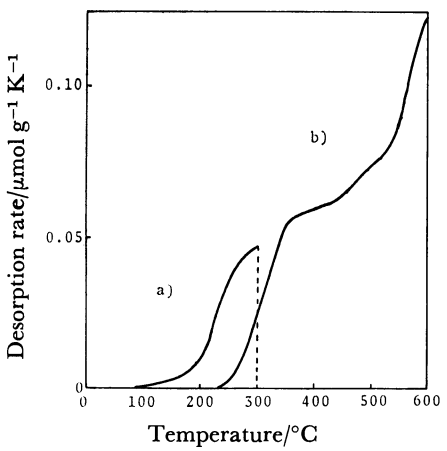

Fig. 7. TPD curues of oxygen from $La_{0.8}Sr_{0.2}CoO_3$.
a): First TPD up to 300 °C, b): second TPD after a) and cooled to room temperature.

The adsorption (and/or absorption) of oxygen at 300 °C was reversible and was saturated at about 10 Torr. When this sample (x=0.2) was cooled to room temperature in oxygen, 0.06 cm^3 g^{-1} of oxygen was adsorbed (absorbed) during the cooling process. The amount of reversible O_2 uptake at room temperature was 2.5×10^{-3} cm^3 g^{-1}, corresponding to a change in δ of 5×10^{-5}, much smaller than the oxygen desorbed in TPD. When the values of δ at 200—300 °C after evacuation (*ca.* 10^{-4} Torr) and under oxygen pressure (*ca.* 10 Torr) (both values increased with x) were plotted against P_{O_2}, difference of several orders of magnitude in the equilibrium pressure of oxygen was found at the same δ value among the samples with different x. Samples having greater x had higher equilibrium pressures of oxygen. That is to say, the chemical potential of lattice oxygen increases enormously with x. This fact confirms again that the results of TPD reflect the chemical potential of lattice oxygen.

As shown in Fig. 2, the release of oxygen from the bulk becomes more difficult for samples calcined at higher temperatures. The result reported previously that the catalytic activities of C_3H_8 oxidation over $La_{0.8}Sr_{0.2}CoO_3$ changed with the calcination temperature and showed a maximum at 850 °C[8] may be explained by the trend seen in TPD of Fig. 2.

In the reduction by CO pulse, the amount of oxygen consumed in one pulse was so large that the CO-pulse experiments reflect mainly the reactivity of lattice oxygen. The conversion of CO increased enormously with x (Table 1) similarly to the trend found with TPD. This similarity between the results of two experiments demonstrates that the reactivity of adsorbed oxygen runs parallel with that of lattice oxygen even if adsorbed

oxygen should exist. It is noted in TPD that the change from oxygen desorbed at low temperature (adsorbed oxygen or weakly bonded lattice oxygen) to oxygen desorbed at higher temperature (lattice oxygen) was continuous and a parallelism was found between the two oxygen species. Probably, it is reasonable not to distinguish between adsorbed and lattice oxygen in the present system.

There was a tendency that re-oxidation became slower on increasing Sr^{2+} substitution, contrary to the case of reduction. The easier reduction and slower re-oxidation with samples having high x mean the equilibrium pressure of oxygen is very much greater for these samples. Actually the equilibrium pressure estimated as above increased tremendously with x. This result will be discussed in more detail in the following paper.

Diffusion of Oxygen in the Bulk and Activation of Oxygen on the Surface. It is known that the diffusion of oxygen in the bulk is rapid in the perovskite-type mixed oxides.[11] We also reported that the diffusion was very rapid during the redox cycle of $La_{0.8}Sr_{0.2}CoO_3$.[22] As shown in Fig. 6b, exchange reaction between gaseous and lattice oxygen occurred under oxygen atmosphere in $La_{1-x}Sr_xCoO_3$, and ^{18}O diffused into the bulk at a considerable rate. The rates of exchange reaction at 150 °C were not so different between $x=0$ and 0.2, 0.0015 $cm^3\ g^{-1}\ min^{-1}$, but the rates at 300 °C were 0.014 $cm^3\ g^{-1}\ min^{-1}$ for $x=0$ and 0.127 $cm^3\ g^{-1}\ min^{-1}$ for $x=0.2$. Sample with $x=0.6$ exhibited a much greater value of 0.045 $cm^3\ g^{-1}\ min^{-1}$, even at 150 °C. Since equilibration was much more rapid and the equilibration usually proceeds *via* dissociation of oxygen in this temperature range, the dissociation of oxygen molecules at the surface is much more rapid than the exchange reaction. Therefore, the rate-determining step of the exchange reaction is probably not the surface reaction but the diffusion in the bulk. The acceleration of the exchange reaction by the Sr^{2+} substitution may be due to the increase in the diffusion rate of oxygen. This is reasonable, if one considers that the diffusion occurs through oxygen vacancies and the amount of the vacancy increases with the Sr^{2+} content. This rapid diffusion of oxygen was revealed also by the results of CO pulse reaction described above.

Finally, the activation of oxygen at the surface will be discussed. The rates of equilibration at 150 °C were 0.037 $cm^3\ g^{-1}\ min^{-1}$ for $x=0$ and 0.35 $cm^3\ g^{-1}\ min^{-1}$ for $x=0.2$. For $x=0.6$ it was not possible to determine the rate of equilibration because of the rapid exchange between gaseous and lattice oxygen even at 150 °C, but the rate appears greater than that for $x=0.2$. Thus, the ability to activate oxygen also increases with x. In $La_{1-x}Sr_xCoO_3$, considerable amount of oxygen vacancies are formed even under oxygen atmosphere as shown in the results of oxygen adsorption, and its amount increased with x. It can therefore be presumed that the equilibration occurs at this surface oxygen defect and the rate becomes faster when the oxygen defects at the surface increases.

Conclusion. In the perovskite-type mixed oxides, $La_{1-x}Sr_xCoO_3$, the reactivity of lattice oxygen, the desorption of oxygen and the reduction tends to become easier as the Sr^{2+} content, x, increases. This is due to the formation of unstable Co^{4+} and the high chemical potential of lattice oxygen. Unstable Co^{4+} changes to Co^{3+}, when oxygen is desorbed and oxygen vacancy is formed. As the vacancy increases, the diffusion of lattice oxygen from bulk to surface becomes easier. In this system, even in an oxygen atmosphere, oxygen vacancies are present and their amount increases with x. This is the reason why the rate of isotopic equilibration of oxygen and exchange between gaseous and lattice oxygen increased with x. Thus, easy formation of oxygen vacancies, keeping its structure unchanged, is the remarkable characteristics of the present mixed oxide system. Relationships between the present results and catalytic activity will be discussed in the following paper.

References

1) R. J. H. Voorhoeve, "Advanced Materials in Catalysis," Academic Press, New York (1977), p. 129.
2) R. J. H. Voorhoeve, J. P. Remeika, P. E. Freeland, and B.T. Mattias, *Science*, **177**, 353 (1972).
3) Y.-F. Yu Yao, *J. Catal.*, **36**, 266 (1975).
4) R. J. H. Voorhoeve, J. P. Remeika, and L. E. Trimble, "The Catalytic Chemistry of Nitrogen Oxides," Plenum Press, New York (1975), p. 215.
5) M. W. Chien, I. M. Pearson, and K. Nobe, *Ind. Eng. Chem., Prod. Res. Dev.*, **14**, 131 (1975).
6) K. Ichimura, Y. Inoue, and I. Yasumori, *Bull. Chem. Soc. Jpn.*, **53**, 3044 (1980).
7) T. Nakamura, M. Misono, and Y. Yoneda, *Shokubai*, **21**, 310 (1979).
8) T. Nakamura, M. Misono, T. Uchijima, and Y. Yoneda, *Nippon Kagaku Kaishi*, **1980**, 1679.
9) G.W. Keulks, *J. Catal.*, **19**, 232 (1970).
10) M. Misono, K. Sakata, F. Ueda, Y. Nozawa, and Y. Yoneda, *Bull. Chem. Soc. Jpn.*, **53**, 648 (1980).
11) T. Kudo, H. Obayashi, and T. Gejo, *J. Electrochem. Soc.*, **122**, 159 (1975).
12) H. Ohbayashi, T. Kudo, and T. Gejo, *Jpn. J. Appl. Phys.*, **13**, 1 (1974).
13) H. Taguchi, M. Shimada, and M. Koizumi, *Mat. Res. Bull.*, **13**, 1225 (1978).
14) G. H. Jonker and J. H. Van Santen, *Physica*, **19**, 120 (1953).
15) B. E. Gushee, L. Katz, and R. Ward, *J. Am. Chem. Soc.*, **79**, 5601 (1957).
16) H. Taguchi, M. Shimada, and M. Koizumi, *J. Solid State Chem.*, **29**, 221 (1979).
17) A. Hashimoto, J. Mizusaki, S. Yamauchi, and K. Fueki, *Preprint 19th Symp. Basic Science of Ceramics*, Nagoya, Japan, **1981**, 88.
18) H. A. Laitenen and L. W. Burdett, *Anal. Chem.*, **23**, 1268 (1951).
19) H. Taguchi, Y. Takeda, F. Kanamaru, M. Shimada, and M. Koizumi, *Acta Crystallogr., Sect. B*, **33**, 1299 (1977).
20) J. J. Janecek and G. P. Wirtz, *J. Am. Ceram. Soc.*, **61**, 242 (1978).
21) M. Iwamoto, Y. Yoda, N. Yamazoe, and T. Seiyama, *J. Phys. Chem.*, **82**, 2564 (1980).
22) K. Sakata, T. Nakamura, M. Misono, and Y. Yoneda, *Chem. Lett.*, **1979**, 273.